Full paper / Mémoire

Synthesis, crystal and electronic structures of the novel Nd$_{12.4}$Mg$_{0.6}$Mo$_{13}$O$_{36}$ compound containing Mo$_{13}$ clusters

Nicolas Barrier [a,1], Régis Gautier [b], Patrick Gougeon [a,*]

[a] *Laboratoire de chimie du solide et inorganique moléculaire, UMR CNRS 6511, université Rennes-1, Institut de chimie de Rennes, avenue du Général Leclerc, 35042 Rennes cedex, France*
[b] *Laboratoire de chimie du solide et inorganique moléculaire, UMR CNRS 6511, École nationale supérieure de chimie de Rennes, Institut de chimie de Rennes, campus de Beaulieu, 35700 Rennes, France*

Abstract

The synthesis, crystal and electronic structures of the novel neodymium reduced molybdenum oxide Nd$_{12.4}$Mg$_{0.6}$Mo$_{13}$O$_{36}$ are presented. This compound crystallizes in the trigonal space group $R3m$: $a = 11.3103(1)$ Å, $c = 21.7465(3)$ Å, $V = 2409.17(4)$ Å^3, $Z = 3$. Refinements yield $R(F^2) = 0.0311$ and w$R(F^2) = 0.0782$ for 3184 unique reflections. The structure is built up from alternating slabs made up of molybdenum forming Mo$_{13}$ clusters, neodymium and oxygen atoms, and slabs only containing neodymium and oxygen atoms. Theoretical calculations were carried out to understand the electronic structure of this compound. Although some Mo–Mo antibonding levels of the molecular orbital diagram of the Mo$_{13}$ cluster are occupied, the high connectivity of architecture prevents some distortions of the cluster. ***To cite this article: N. Barrier et al., C. R. Chimie 8 (2005).***
© 2005 Académie des sciences. Published by Elsevier SAS. All rights reserved.

Résumé

La synthèse, les structures cristalline et électronique du nouvel oxyde de molybdène réduit et de néodyme, Nd$_{12.4}$Mg$_{0.6}$Mo$_{13}$O$_{36}$, sont présentées. Ce composé cristallise dans le groupe spatial trigonal $R3m$: $a = 11.3103(1)$ Å, $c = 21.7465(3)$ Å, $V = 2409.17(4)$ Å^3, $Z = 3$. Les affinements conduisent aux facteurs de confiance $R(F^2) = 0.0311$ et w$R(F^2) = 0.0782$ pour 3184 réflexions uniques. La structure est construite à partir d'une alternance de couches constituées d'atomes de néodyme, d'oxygène et de molybdène formant des clusters Mo$_{13}$ et de couches ne contenant que des atomes de néodyme et d'oxygène. Des calculs théoriques ont été mis en œuvre afin de comprendre la structure électronique de ce composé. Bien que des niveaux antiliants Mo–Mo du diagramme d'orbitales moléculaires du cluster Mo$_{13}$ soient occupés, la grande connectivité de l'architecture l'empêche de se déformer. ***Pour citer cet article : N. Barrier et al., C. R. Chimie 8 (2005).***
© 2005 Académie des sciences. Published by Elsevier SAS. All rights reserved.

* Corresponding author.
E-mail address: Patrick.Gougeon@univ-rennes1.fr (P. Gougeon).
[1] Present address: Laboratoire Crismat–Ensicaen, 6, bd du Maréchal-Juin, 14050 Caen cedex, France.

1. Introduction

The structural chemistry of compounds containing reduced molybdenum has grown tremendously over the last two decades so that 22 different types of discrete molybdenum clusters, of which the nuclearities goes from 3 to 36, are known to date. Clusters with nuclearities higher than 8 result generally from the one-dimensional condensation of Mo_6 clusters via opposite face- or edge-sharing depending on the ligand environment. The former process is observed when the Mo_6 clusters are face-bridged by the ligands (S, Se and Te) and is exemplified, in particular, by the series of compounds $M_{n-2}Mo_{3n}X_{3n+2}$ (M = Rb, Cs; X = S, Se or Te; n = 3, 4, 5, 6, 7, 8, 10 and 12) containing Mo_{3n} clusters [1–8]. The final stage of this face-sharing condensation is the infinite $\left|Mo_{6/2}\right|_\infty^1$ chain found in the quasi-one-dimensional compounds $M_2Mo_6X_6$ (M = Na, K, Rb, Cs; X = S, Se or Te) [9] and Ag Mo_6Te_6 [44]. The edge-sharing condensation of Mo_6 octahedra is observed in reduced molybdenum oxides where the Mo_6 clusters are edge-bridged by the oxygen atoms. This process leads to Mo_{4n+2} oligomers that are observed for example in the series $M_{n-x}Mo_{4n+2}O_{6n+4}$ (n = 2, 3, 4 and 5) [10–21]. The ultimate step of the edge-sharing-condensation process corresponds to the infinite $\left|Mo_2Mo_{4/2}\right|_\infty^1$ chain of trans-edge-sharing Mo_6 octahedra that was first observed in $NaMo_4O_6$ [22]. More recently, two original high-nuclearity molybdenum clusters, i.e. Mo_{13} and Mo_{19}, were observed in coexistence with the common triangular Mo_3 and the planar Mo_7 clusters in the atypical compound $Pr_4Mo_9O_{18}$ [23]. Contrary to the previous high nuclearity molybdenum clusters, the Mo_{13} and Mo_{19} result, for the first time in solid-state chemistry, from the bi- or tri-dimensional condensation of octahedral Mo_6 clusters, respectively. We present here the synthesis, and the crystal and electronic structures of the first compound containing only Mo_{13} clusters: $Nd_{12.4}Mg_{0.6}Mo_{13}O_{36}$.

2. Experimental section

2.1. Synthesis

Single crystals of $Nd_{12.4}Mg_{0.6}Mo_{13}O_{36}$ were obtained in an attempt to synthesize a phase $MgNd_{16}Mo_{20}O_{56}$ isostructural with $Nd_{16}Mo_{21}O_{56}$ [24]. Starting reagents were La_2O_3 (Rhône-Poulenc, 99.999%), MoO_3 (Strem Chemicals, 99.9%) and Mo (Cimebocuze, 99.9%), all in powder form. The rare-earth oxide was prefired at 1000 °C before use and the Mo powder was heated under a hydrogen flow at 1000 °C for 6 h. The stoichiometric mixture was pressed into a ca. 5 g pellet and loaded into a molybdenum crucible (depth: 2.5 cm; diam: 1.5 cm) which was previously cleaned by heating at 1500 °C for 15 min under a dynamic vacuum of about 10^{-5} Torr and then sealed under a low argon pressure using an arc welding system. The crucible was heated at a rate of 300 °C h^{-1} to 1600 °C and held there for 3 days, then cooled at 100 °C h^{-1} to 1100 °C and finally furnace cooled to room temperature

2.2. Single crystal structure determination

A black crystal of dimensions 0.26 × 0.060 × 0.026 mm^3 was selected for data collection. Intensity data were collected on a Nonius Kappa CCD diffractometer using a graphite-monochromatized Mo Kα radiation (λ = 0.71073 Å) at room temperature. The COLLECT program package [25] was used to establish the angular scan conditions (φ and ω scans) used in the data collection. The data set was processed using Eval-CCD [26] for the integration procedure. An absorption correction (T_{min} = 0.01131, T_{max} = 0.2315) was applied using the description of the crystal faces and the analytical method described by de Meulenaar and Tompa [27]. The structure was solved by direct methods using Sir97 [28] and subsequent difference Fourier syntheses in the space group R3 m. All structure refinements and Fourier syntheses were carried out using SHELXL-97 [29]. Refinement of the occupancy factors of the Nd sites showed that the Nd2, Nd3 and the Nd5 sites are slightly deficient and occupy at 98.6 (4)%, 0.972 (4)% and 0.98 (5)%, respectively. As qualitative microanalyses using a JEOL JSM-35 CF scanning electron microscope equipped with a Tracor energy-dispersive-type X-ray spectrometer indicated the presence of magnesium in the crystals, we could expect that the deficiencies observed on some of the Nd sites results from the presence of magnesium since in the final difference Fourier map we did not observed peaks compatible with Mg positions. Refinements taking into account an occupation of the deficient Nd sites simultaneously by Nd and Mg atoms were unsuccessful. However, if assume a complete occupation of the Nd2,

Nd3 and Nd5 sites by Nd and Mg atoms, we get the composition $Nd_{12.4(1)}Mg_{0.6(1)}Mo_{13}O_{36}$ which is in good agreement with that found by I.C.P. measurement, $Nd_{12.5(3)}Mg_{0.51(5)}Mo_{13.11(4)}O_{36}$. The positional and anisotropic displacement parameters for all atoms as well as the occupancy factors for the Nd atoms were refined to the values $R_1 = 0.0311$, w$R_2 = 0.0782$ for 126 parameters and 3184 reflections with $I > 2\,\sigma(I)$ and the residual electron densities were 3.310 and

-3.517 e $\mathring{A}^{-3}$. A summary of the X-ray crystallographic and experimental data are presented in Table 1, and selected interatomic distances are reported in Table 2.

2.3. Theoretical calculations

Extended Hückel [30] molecular calculations were carried out using the program CACAO [31]. The exponents (ζ) and the valence shell ionization potentials (H_{ii} in eV) used were, respectively: 2.275, –32.3 for O 2s; 2.275, –14.8 for O 2p; 1.956, –8.34 for Mo 5s; 1.921, –5.24 for Mo 5p; 2.14. The H_{ii} value for Mo 4d was set equal to –10.50. A linear combination of two Slater-type orbitals of exponents $\zeta_1 = 4.542$ and $\zeta_2 = 1.901$ with equal weighting coefficients was used to represent the Mo 4d atomic orbitals.

Self-consistent ab initio band structure calculations were performed on the model compound $Nd_{13}Mo_{13}O_{36}$ with the scalar relativistic tight-binding linear muffin-tin orbital (LMTO) method in the atomic spheres approximation including the combined correction [32–36].

Table 1
Experimental table

Chemical formula	$Nd_{12.4}Mg_{0.6}Mo_{13}O_{36}$
M_r	3671.42
Cell setting, space group	Trigonal, $R3m$
a, c (Å)	11.3103 (1), 21.7465 (3)
V (Å^3)	2409.17 (4)
Z	3
D_x (Mg m^{-3})	7.592
Radiation type	Mo $K\alpha$
Number of reflections for cell parameters	16,985
θ Range (°)	1.0–37.8
μ (mm^{-1})	24.62
Temperature (K)	293 (2)
Crystal form, color	Truncated hexagonal block, black
Crystal size (mm)	$0.26 \times 0.06 \times 0.03$
Diffractometer	KappaCCD
Data collection method	φ and ω scans
Absorption correction	Analytical
T_{min}	0.011
T_{max}	0.232
Number of measured, independent and observed parameters	23,571, 3203, 3184
Criterion for observed reflections	$I > 2\sigma(I)$
R_{int}	0.072
θ_{max} (°)	37.8
Range of h, k, l	$-18 \rightarrow h \rightarrow 19/-19 \rightarrow k \rightarrow 19/-37 \rightarrow l \rightarrow 37$
Refinement on	F^2
$R[F^2 > 2\sigma(F^2)]$, w$R(F^2)$, S	0.031, 0.078, 1.09
Number of reflections	3203 reflections
Number of parameters	126
Weighting scheme	Calculated $w = 1/[\sigma^2(F_o^2) + (0.0354\,P)^2 + 109.0437\,P]$ where $P = (F_o^2 + 2\,F_c^2)/3$
$(\Delta/\sigma)_{max}$	0.095
$\Delta\rho_{max}$, $\Delta\rho_{min}$ (e Å^{-3})	3.31, –3.52
Extinction method	SHELXL
Extinction coefficient	0.000255 (19)

Table 2
Selected interatomic distances (Å) for $Nd_{12.4}Mg_{0.6}Mo_{13}O_{36}$

|			
Nd1–O2 (×6)	2.832 (5)	Nd4–O3	2.836 (8)
Nd1–O4	2.339 (11)	Nd4–O4	2.373 (4)
Nd1–O5 (×3)	2.406 (7)	Nd4–O6 (×2)	2.345 (5)
Nd2/Mg–O1 (×2)	2.773 (4)	Nd4–O7 (×2)	2.883 (5)
Nd2/Mg–O10	2.345 (9)	Nd4–O8 (×2)	2.400 (5)
Nd2/Mg–O11	2.148 (2)	Nd5/Mg–O10	2.318 (11)
Nd2/Mg–O2 (×2)	2.437 (5)	Nd5/Mg–O5 (×2)	2.330 (4)
Nd2–O6 (×2)	2.441 (5)	Nd5/Mg–O6 (×2)	2.329 (5)
Nd3/Mg–O1	2.903 (6)	Nd5/Mg–O9	2.928 (7)
Nd3/Mg–O10 (×2)	2.316 (6)	Nd5′/Mg–O10	2.834 (19)
Nd3/Mg–O7	2.332 (6)	Nd5′/Mg–O5 (×2)	2.214 (9)
Nd3/Mg–O8 (×2)	2.464 (5)	Nd5′/Mg -O6 (×2)	2.200 (9)
Nd3/Mg–O9 (×2)	2.633 (5)		
Mo1–Mo2 (×6)	2.7324 (5)	Mo4–Mo3	2.7567 (6)
Mo2–Mo2	2.6918 (10)	Mo1–Mo4 (×3)	2.8478 (12)
Mo2–Mo2	2.7715 (9)	Mo2–Mo4	2.7858 (7)
Mo3–Mo2 (×2)	2.7137 (7)	Mo3–Mo4	2.7566 (6)
Mo4–Mo2	2.7858 (7)	Mo3–Mo4	2.7566 (6)
Mo2–Mo3	2.7137 (7)	Mo4–Mo4 (×2)	2.7471 (12)
Mo4–Mo3	2.7566 (6)		
Mo1–O9 (×3)	2.128 (7)	Mo3–O2 (×2)	1.969 (5)
Mo2–O1	2.135 (5)	Mo3–O5	2.101 (6)
Mo2–O2	2.076 (5)	Mo3–O8 (×2)	2.065 (5)
Mo2–O6	2.043 (5)	Mo4–O1	2.119 (6)
Mo2–O7	2.079 (5)	Mo4–O3	2.079 (8)
Mo2–O9	2.122 (5)	Mo4–O8 (×2)	2.105(5)
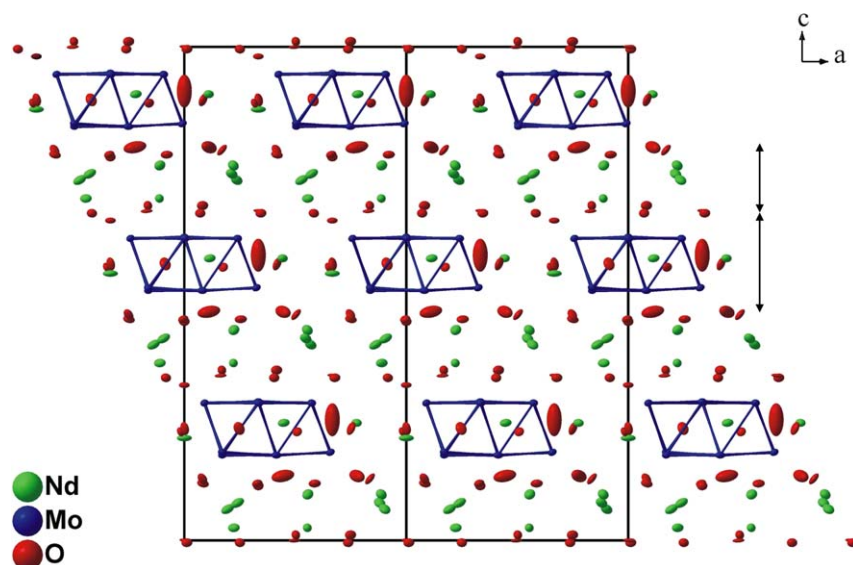
Fig. 1. A perspective view of the crystal structure of $Nd_{12.4}Mg_{0.6}Mo_{13}O_{36}$ along the b axis.

Exchange and correlation were treated in the local density approximation using the von Barth and Hedin [37] local exchange correlation potential. Within the LMTO formalism interatomic spaces are filled with interstitial spheres. The optimal positions and radii of these additional 'empty spheres' were determined by the proce-

dure described in Ref. [38]. Twenty-four non-symmetry-related 'empty spheres' with 0.62 Å $\leq r_{ES} \leq 1.60$ Å were introduced for the calculations. The full LMTO basis set consisted of 6s, 6p, 5d and 4f functions for Nd spheres, 5s, 5p, 4d and 4f functions for Mo spheres, 2s, 2p and 3d functions for O spheres, and s, p and d functions for 'empty spheres'. The eigenvalue problem was solved using the following minimal basis set obtained from the Löwdin downfolding technique: Nd 6s, 5d, 4f, Mo 5s, 5p, 4d, O 2s, 2p and interstitial 1s LMTOs. The k space integration was performed using the tetrahedron method [39]. Charge self-consistency and the average properties were obtained from 46 irreducible k points. A measure of the magnitude of the
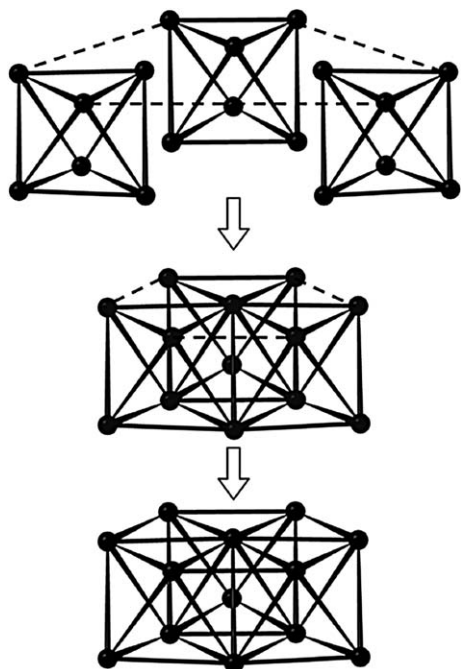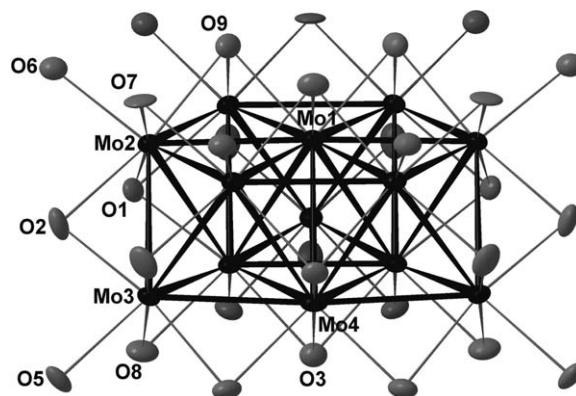

Fig. 2. Condensation process for the Mo_{13} cluster.

Fig. 3. The Mo_{13} cluster with its oxygen environment (97% probability ellipsoids).
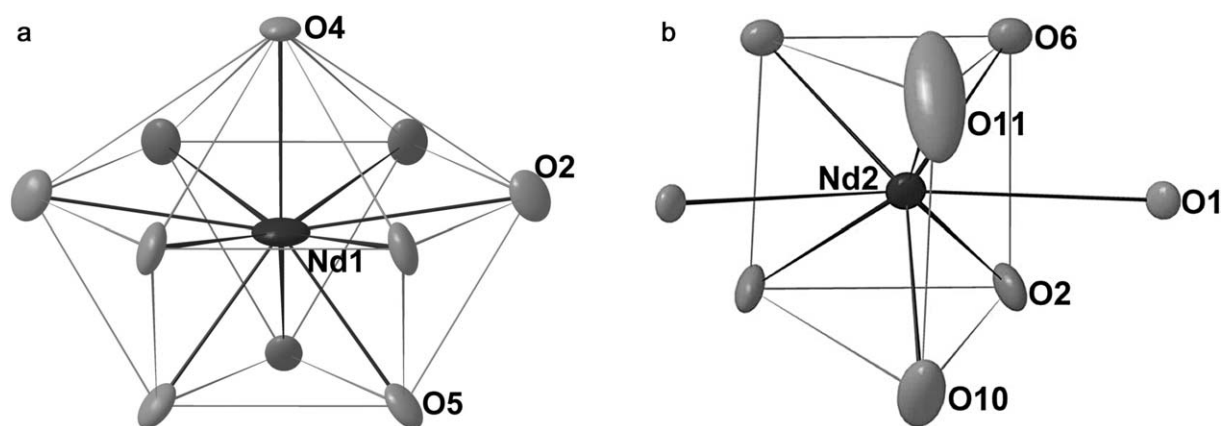
Fig. 4. Oxygen environments for the Nd1 and Nd2 atoms.

bonding was obtained by computing the crystal orbital Hamiltonian populations (COHP) which are the Hamiltonian population weighted density of states (DOS) [40]. As recommended [41], a reduced basis set (in which all ES LMTO's have been downfolded) was used for the COHP calculations. DOS and COHP curves are shifted so that ϵ_F lies at 0 eV.

3. Results and discussion

3.1. Structure description

A perspective view of the crystal structure of $Nd_{12.4}Mg_{0.6}Mo_{13}O_{36}$ along the *b* axis is represented in Fig. 1. It shows that this structure can be viewed as a stacking along the *c*-axis of two different slabs interconnected through oxygen atoms. The A slab is made up of molybdenum forming Mo_{13} clusters, neodymium and oxygen atoms, and the B slab of neodymium and oxygen atoms.

In the A slab, the Mo_{13} cluster is similar to that encountered in the compound $Pr_4Mo_9O_{18}$. It has 3 m (C_{3v}) symmetry and may be regarded as resulting from the edge-sharing-condensation of three Mo_6 octahedra having the same apex in common, as depicted in Fig. 2. The Mo–Mo bond distances within the Mo_{13} cluster range from 2.692(1) to 2.848(1) Å with an average value of 2.74 Å and are thus quite comparable to those found
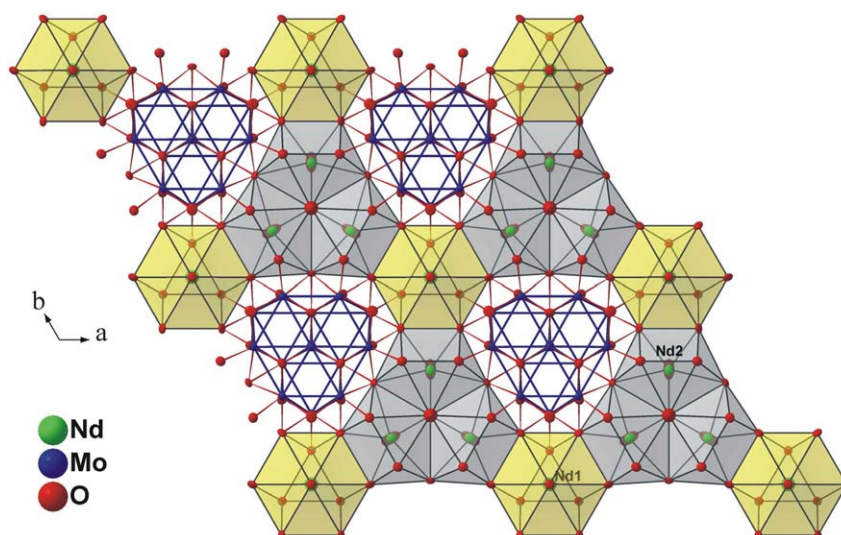

Fig. 5. A polyhedral representation of the A slab viewed along the *c* axis.

in one-dimensional condensed Mo clusters. The molybdenum atoms are linked to three (Mo1), four (Mo4) or five (Mo2, Mo3) oxygen atoms. These bridge the Mo-Mo edges (O2, O7, O8), cap the triangular Mo faces (O1, O4, O9) or are bonded exo to the Mo apices of the Mo_{13} polyhedron (O5, O6) leading to the $Mo_{13}O_{31}$ unit shown in Fig. 3. The Mo–O bond distances lie between 1.969(5) and 2.135(5) Å with an average value of 2.08 Å. In the A slab, we also find the neodymium atoms Nd1 and Nd2 that are surrounded by 10 and 8 oxygen atoms, respectively. The coordination polyhedra around both neodymium atoms are shown in Fig. 4. The $Nd1O_{10}$ polyhedron may be described as the stacking of a triangle formed by the O5 on a hexagon of O2 atoms which is capped by the O4 atom. The environment of the Nd2 atoms may be viewed as a distorted bicapped trigonal prism. The Nd–O distances range from 2.339(11) to 2.832(5) for the Nd1 site and from 2.148(2) to 2.774(4) for the Nd2 site. The arrangement of the $Mo_{13}O_{31}$ units and the $Nd1O_{10}$ and $Nd2O_8$ polyhedra in the A slab is shown in Fig. 5.

In the B slab, we find the remaining Nd atoms, i.e. Nd3, Nd4, Nd5 and Nd5′ (Fig. 6). The Nd3 and Nd4 atoms are eight-coordinate in oxygen but present different environments. Nd3has a bicapped trigonal prismatic environment and Nd4 is at the center of a tricapped square-based pyramid. The Nd3–O bond distances lie between 2.331(6) and 2.904(6) Å and the Nd4–O between 2.345(5) and 2.883(5) Å. The last Nd atom is delocalized over two the two positions Nd5 and Nd5′ in a monocapped square-based pyramid. The Nd5–O and Nd5′–O distances vary between 2.313(11) and 2.927(7) Å and between 2.210(17) and 2.750(10) Å, respectively. The Fig. 7 shows the arrangement of the $Nd3O_8$, $Nd4O_8$ and (Nd5, Nd5′) O_6 polyhedra within the B slab.

3.2. Bond-length bond-strength formula

The estimation of the oxidation states of molybdenum and, consequently, of the number of electrons per Mo_{13} cluster could be performed on this compound using the empirical bond length-bond strength relationship developed by Brown and Wu [42] for Mo–O bonds:

$$s(Mo - O) = [d(Mo - O)/1.882]^{-6}$$

In the above formula, s(Mo–O) is the bond-strength in valence units, d(Mo–O) is the observed Mo–O bond
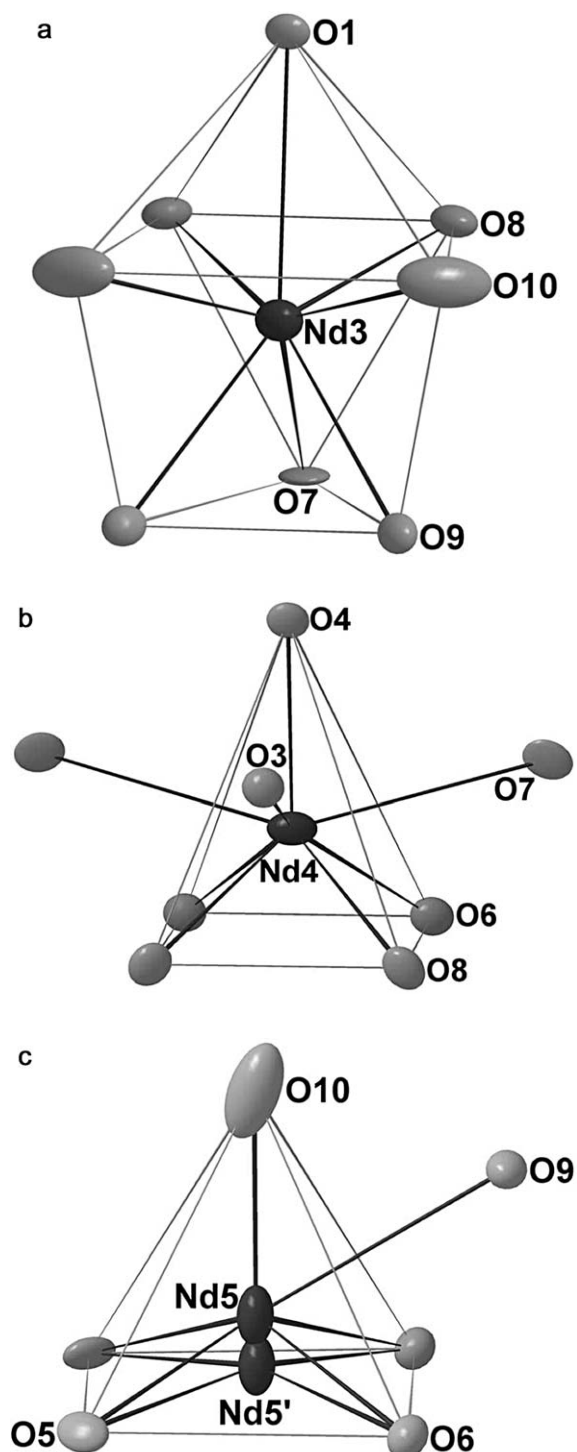

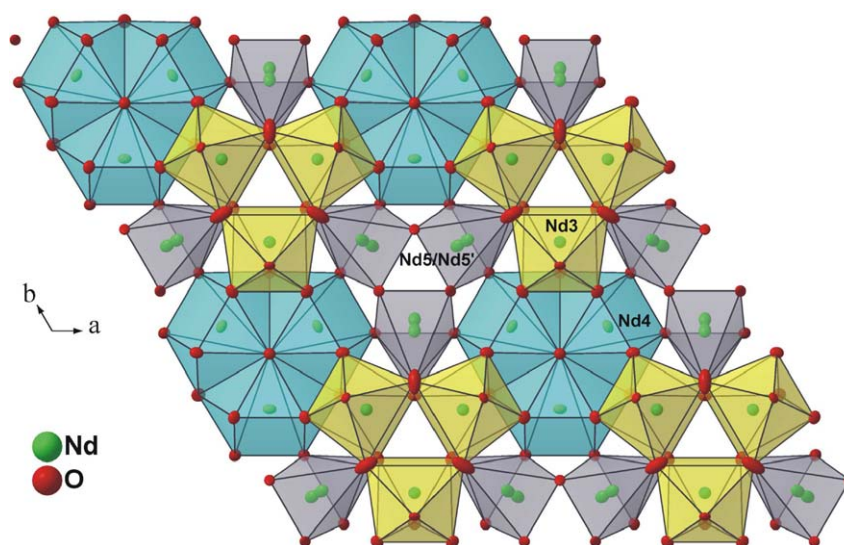Fig. 6. Oxygen environments for the Nd3, Nd4 and Nd5 atoms.

Fig. 7. A polyhedral representation of the B slab viewed along the *c* axis.

distance in Å, 1.882 Å corresponds to a Mo–O single bond distance, and the exponential parameter-6 is characteristic of the Mo atom. Thus, the sum of the Mo–O bond strengths *s* (in valence units) about a particular Mo atom is equal to the oxidation state of that Mo atom. For the four crystallographically independent Mo atoms, these calculations lead to the number oxidation states of +1.44(2), 2.67(4), 3.19(5) and +2.06(3) for Mo1, Mo2, Mo3 and Mo4, respectively. From these values, we could estimate the metallic electron (ME) count per Mo_{13} cluster to 44.7(4), which is in good agreement with the value of 44.4(3) e^- based on the stoichiometry.

3.3. Electronic structure

Extended Hückel calculations were performed on the experimental $Mo_{13}O_{31}$ cluster of C_{3v} symmetry. The corresponding molecular orbital (MO) diagram is shown in Fig. 8. Because of the electronegativity difference of molybdenum and oxygen atoms, MOs that lie in the HOMO/LUMO part of MO diagram shows a major metallic d character. The 48e, 49e and $33a_1$ MOs show an overall Mo–Mo non-bonding character as revealed by the metal–metal overlap populations examination, whereas lower and higher metallic MOs are Mo–Mo bonding and antibonding, respectively. The 48e, 49e and $33a_1$ MOs become the HOMO for the ME count of 42, 46, and 48, respectively. No well-defined
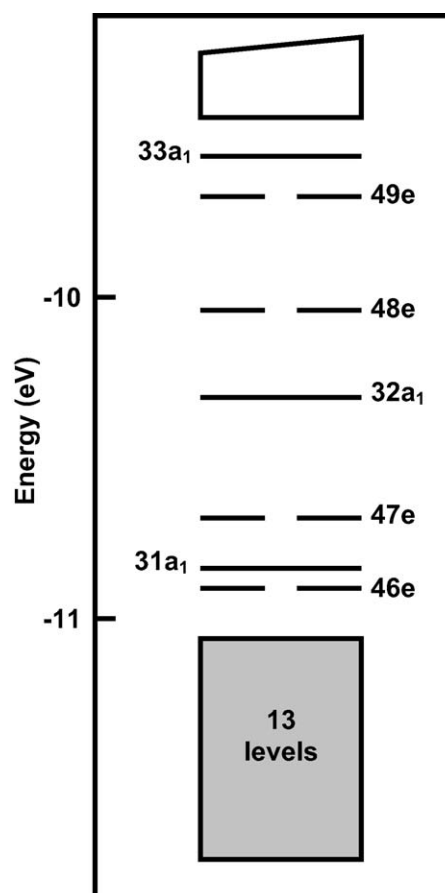

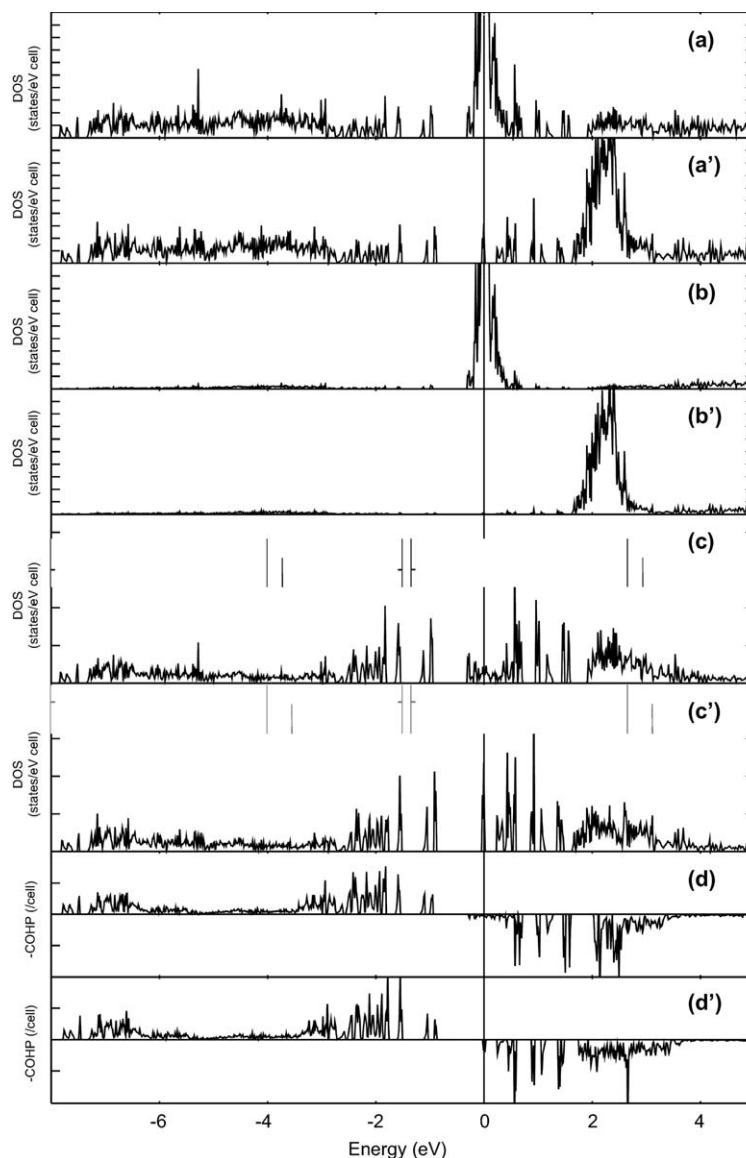Fig. 8. Extended Hückel molecular orbital diagram of $Mo_{13}O_{31}$.

Fig. 9. Spin-polarized DF calculations for the model compound $Nd_{13}Mo_{13}O_{36}$: (a) spin-up and (a′) spin-down total DOS, (b) spin-up and (b′) spin-down Nd projected DOS, (c) spin-up and (c′) spin-down Mo projected DOS, (d) spin-up and (d′) spin-down averaged COHP for Mo–Mo bonds of the cluster.

HOMO/LUMO gaps are observed for those ME counts. Such a situation has been frequently encountered for metal clusters with a high metal–metal connectivity [43]. Spin-polarized periodic density functional (DF) calculations were carried out on the model compound $Nd_{13}Mo_{13}O_{36}$ where no Mg atoms are considered and all Nd5 and Nd5′ positions are fully occupied and vacant, respectively. Since no close metal–metal contacts are observed between the Mo_{13} clusters in the crys-

tal, no significant perturbation of the Mo_{13} clusters' MO pattern is expected in the three-dimensional solid. Spin-polarized total, Nd and Mo projected DOS and Mo–Mo COHP are sketched in Fig. 9. The Fermi level cuts a spin-up DOS peak mainly centered on Nd 4f. Since three electrons occupy this DOS peak inducing a + 3 oxidation state for the Nd atoms, the ME count of the Mo_{13} cluster is equal to 45. The Fermi level cuts also a rather large Mo projected spin-up DOS peak and a nar-

row Mo projected spin-down DOS peak that are both weakly Mo–Mo antibonding. Theses bands are separated by an energy of more than half an eV from lower Mo–Mo bonding bands. Assuming a rigid band model, this gap becomes the band gap for the ME count of 42. Although some Mo–Mo antibonding bands are occupied, the C_{3v} symmetry architecture is preserved for this cluster because of the high connectivity of the different atoms constituting the cluster. Periodic DF calculations suggest that an open-shell configuration is encountered for the $Mo_{13}O_{31}$ unit in this model compound. Because of the absence of significant HOMO/LUMO gaps, strong Jahn–Teller distortions of the cluster could occur for the low spin state configuration that is less stable than the high spin state. Magnetic properties consistent with the presence of Nd^{3+} and some polarized electrons on Mo atoms are expected.

4. Supplementary material

Further details of the crystal structure investigation may be obtained from the Fachinformationszentrum Karlsruhe, D-76344 Eggenstein-Leopoldshafen, Germany (Fax: +49 7247 808 666; e-mail: crysdata@fiz-karlsruhe.de), on quoting the depository number CSD-414275.

References

[1] P. Gougeon, J. Padiou, J.Y. Le Marouille, M. Potel, M. Sergent, Solid-State Chem. 51 (1984) 218.
[2] P. Gougeon, M. Potel, J. Padiou, M. Sergent, Mater. Res. Bull. 22 (1988) 1087.
[3] P. Gougeon, M. Potel, M. Sergent, Acta Crystallogr. C 45 (1989) 182.
[4] P. Gougeon, M. Potel, M. Sergent, Acta Crystallogr. C 45 (1989) 1413.
[5] P. Gougeon, M. Potel, J. Padiou, M. Sergent, Mater. Res. Bull. 23 (1988) 453.
[6] P. Gougeon, M. Potel, M. Sergent, Acta Crystallogr. C 46 (1990) 2284.
[7] S. Picard, P. Gougeon, M. Potel, Acta Crystallogr. C 53 (1997) 1519.
[8] P. Gougeon, PhD thesis, Rennes, 1984.
[9] M. Potel, PhD thesis, Rennes, 1981.
[10] S.J. Hibble, A.K. Cheetham, A.R.L. Bogle, H.R. Wakerley, D.E.J. Cox, Am. Chem. Soc. 110 (1988) 3295.
[11] R. Dronskowski, A. Simon, Angew. Chem. Int. Ed. Engl. 28 (1989) 758.
[12] P. Gougeon, M. Potel, M. Sergent, Acta Crystallogr. C 46 (1990) 1188.
[13] P. Gougeon, P. Gall, M. Sergent, Acta Crystallogr. C 47 (1991) 421.
[14] R. Dronskowski, A. Simon, W.Z. Mertin, Anorg. Allg. Chem. 602 (1991) 49.
[15] P. Gougeon, P. Gall, Acta Crystallogr. C 50 (1994) 7.
[16] P. Gougeon, P. Gall, Acta Crystallogr. C 50 (1994) 1183.
[17] R. Dronskowski, A. Simon, Acta Chem. Scand. A 45 (1991) 850.
[18] G.L. Schimek, S.C. Chen, R.E. Mc Carley, Inorg. Chem. 34 (1995) 6130.
[19] G.L. Schimek, D.A. Nagaki, R.E. Mc Carley, Inorg. Chem. 33 (1994) 1259.
[20] R. Dronskowski, H.J. Mattausch, A. Simon, Zeit. Anorg. Allg. Chem. 619 (1993) 1397.
[21] G.L. Schimek, R.E. Mc Carley, J. Solid-State Chem. 113 (1994) 345.
[22] C.C. Torardi, R.E. Mc Carley, J. Am. Chem. Soc. 101 (1979) 3963.
[23] J. Tortelier, P. Gougeon, Inorg. Chem. 37 (1998) 6229.
[24] P. Gall, P. Gougeon, Z. Krist. 213 (1998) 1.
[25] B.V. Nonius, COLLECT, data collection software, Nonius BV, 1999.
[26] A.J.M. Duisenberg, Reflections on Area Detectors, PhD thesis, Utrecht, 1998.
[27] J. de Meulenaar, H. Tompa, Acta Crystallogr. A 19 (1965) 1014.
[28] A. Altomare, M.C. Burla, M. Camalli, G.L. Cascarano, C. Giacovazzo, A. Guagliardi, A.G.G. Moliterni, G. Polidori, R.J. Spagna, Appl. Crystallogr. 32 (1999) 115.
[29] G.M. Sheldrick, SHELXL 97, Program for the Refinement of Crystal Structures, University of Göttingen, Germany, 1997.
[30] R. Hoffmann, J. Chem. Phys. 39 (1963) 1397.
[31] C. Mealli, D. Proserpio, J. Chem. Educ. 67 (1990) 399.
[32] O.K. Andersen, Phys. Rev. B 12 (1975) 3060.
[33] O.K. Andersen, Europhys. News 12 (1981) 4.
[34] O.K. Andersen, O. Jepsen, Phys. Rev. Lett. 53 (1984) 2571.
[35] O.K. Andersen, O. Jepsen, M. Sob, in: M. Yussouf (Ed.), Electronic Band Structure and its Application, Springer-Verlag, Berlin, 1986.
[36] H.L. Skriver, The LMTO Method, Springer-Verlag, Berlin, 1984.
[37] U. von Barth, L. Hedin, J. Phys. C 5 (1972) 1629.
[38] O. Jepsen, O.K. Andersen, Z. Phys. B 97 (1995) 35.
[39] P.E. Blöchl, O. Jepsen, O.K. Andersen, Phys. Rev. B 49 (1994) 16223.
[40] R. Dronskowski, P.E. Blöchl, J. Phys. Chem. 97 (1993) 8617.
[41] O. Jepsen, O.K. Andersen, personal communication.
[42] I.D. Brown, K.K. Wu, Acta Crystallogr. B 32 (1976) 1957.
[43] R. Gautier, J.-F. Halet, J.-Y. Saillard, in: P. Braustein, L.A. Oro, P.R. Raithby (Eds.), Metal Clusters in Chemistry, VCH, Weinheim, Germany, 1999, p. 1643.
[44] P. Gougeon, M. Potel, J. Padiou, M. Sergent, J. Solid-State Chem. 68 (1987) 137.